International Journal of the Physical Sciences Vol. 6(15), pp. 3745-3753, 4 August, 2011
Available online at http://www.academicjournals.org/IJPS
DOI: 10.5897/IJPS11.774
ISSN 1992-1950 ©2011 Academic Journals

Full Length Research Paper

The effect of magnetic impurity on the electronical and optical properties of corundum

H. A. Rahnamaye Aliabad[1], N. Mahmoodi[2] and H. Arabshahi[3,4]*

[1]Department of Physics, Sabzevar Tarbiat Moallem University, Sabzevar, Iran.
[2]Department of Physics, Azad university of Mashhad, Mashhad, Iran.
[3]Department of Physics, Ferdowsi University of Mashhad, Mashhad, Iran.
[4]Department of Physics, Payame Nour University of Fariman, Fariman, Iran.

Accepted 30 June, 2011

We have studied the structural, electronical and optical properties of pure α-Al_2O_3 (corundum) and doped with manganese by the first principles calculations method based on the density functional theory (DFT), with generalized gradient approximation (GGA). Obtained results show that α-Al_2O_3 has an energy gap of 6.3 eV and the substitution of manganese decreases the energy gap so that spin splitting effect is observed. Calculated optical results show that with adding this impurity, reflectivity increase at low energy and decreases at high energy; also static refractive index increases.

Key words: Corundum, manganese, density functional theory (DFT), energy gap, refractive index.

INTRODUCTION

Alumina is one of the most interesting materials at industry and it has high importance because of its hardness, useful optical properties, abrasion resistance, mechanical strength, and electronical and optical properties (Ahuja et al., 2004). It has different phases such as, α, β, γ, χ so that the α-phase is the permanent and suitable condition for the industrial applications that there are some good studies in both fields, experimental and theoretical (Wang et al., 2005). In this article, we bear in mind the α-phase of this compound that is called corundum. Today, for understanding the electronical and optical properties of this material, first principles calculations have great usage. For optimizing of these properties, we tried to study the electronical and optical properties of this compound with doping Mn magnetic impure. We study the effect of Mn's spin polarization on electronical and optical properties α-Al_2O_3. The structure of α–Al_2O_3 is rhombohedral that consists of close-packed planes of oxygen and aluminium. Its space group is R-3c with number 167. There are 12 Al atoms and 18 O atoms (30 atoms) in the unit cell of α –Al_2O_3 (Peterson et al., 2000). Mn atoms, which have the same valence with Al (+3), are substitute at octahedral sites within the alumina structure in the Al sites (Figure 1). For calculation of lattice constants, lattice energy variation as a function of the deviation of c/a (ratio, %) in constant volume have been calculated from experimental values for α-$Al_{1.5}Mn_{0.5}O_3$. These results are shown in Table 1. It can be seen that our results is in good agreement with experimental results for α-Al_2O_3. Then with calculated lattice constants, relaxed atomic positions were obtained for α-Al_2O_3 and α-$Al_{1.5}Mn_{0.5}O_3$. The obtained results are based on relaxed parameters.

METHOD OF CALCULATIONS

In our calculations, we have used density functional theory (DFT) based on the work by Hohenberg and Kohn and by Kohn and Sham (2011). Self-consistent electron structures were performed using the full potential linearized augmented plane wave (FP-LAPW) method as implemented in WIEN2K code (Blaha et al., 2011). We have also used the generalized gradient approximation (GGA) for the exchange-correlation interaction (Chatterjee et al., 2005). For solving the Kohn-Sham equations, the relativistic effects have been taken into account. In our calculations, we selected the parameter that determines the size of the secular matrix to be: RMT * K_{max} = 7 where the RMT is Muffin-Tin sphere radii and K_{max} is the cut-off wave vector in the first B.Z. The iteration process was stopped after the calculated total energy converged to less than 0.0001 Ry. The

*Corresponding author. Email: hadi_arabshahi@yahoo.com.

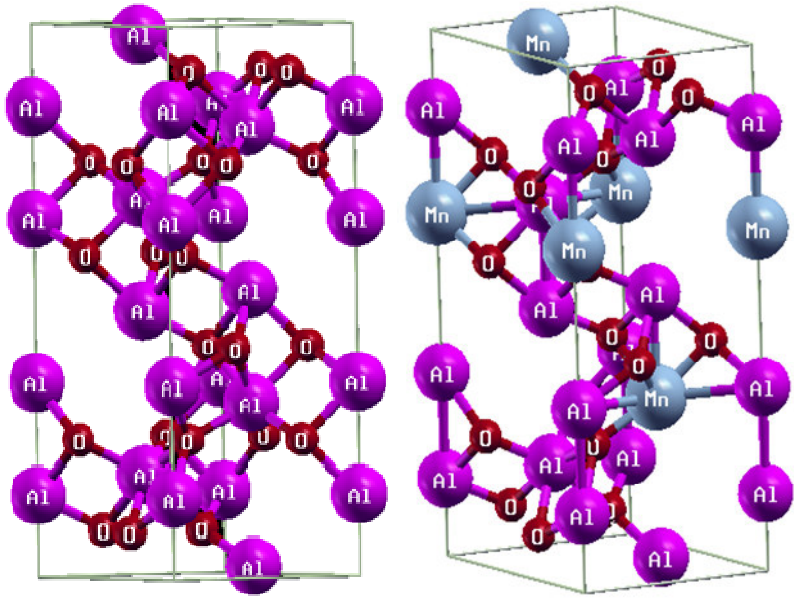

Figure 1. The unit cells of (a) pure α -Al_2O_3 and (b) α-$Al_{1.5}Mn_{0.5}O_3$ used in this study.

Table 1. Calculated lattice constants for α –Al_2O_3 and α–$Al_{1.5}Mn_{0.5}O_3$.

Compound	This work(Å)	Others (Experiment Å)
α –Al_2O_3	a = b = 4.758 c = 12.981	a = b = 4.761 c = 12.991
α –$Al_{1.5}Mn_{o.5}O_3$	a = b = 4.759 c = 12.974	- -

LAPW+LO method is used, because for Mn element is suitable and it has localized d states.

RESULTS AND DISCUSION

Electronical results

Band structure and band gap

The calculated band structure for α-Al_2O_3 has been shown in Figure 2. Fermi energy has considered on the top of the valence band. On the top of the valence band, O 2p orbital has the most contribution and at the bottom of conduction band there are O 2p, Al 2s and Al 2p orbital's. The obtained energy gap is 6.3 eV that had been compared with the theoretical and experimental results of others in Table 2. The calculated band structure for α-$Al_{1.5}Mn_{0.5}O_3$, with spin-up and spin-down have been shown in Figure 3. In these two cases, the energy gap, decreases in both states. The band gap in both states is indirect and is equal to 3.7 eV for the spin-down and 0.6 eV for spin-up. In spin-up valence band, Mn 3d and Al 3p orbitals and for its conduction band Al 3p orbitals have the most portions. Spin splitting is seen at the figures obviously. It is very interesting that energy gap also change without the spin polarization effect. Calculated band gap for α-$Al_{1.5}Mn_{0.5}O_3$ without spin effect is shown in Figure 4. In this case, obtained band gap is 2.5 eV and this value is very different with before states. Therefore spin polarization effect is playing important role in calculation of electronical properties of this compound.

Density of states

Electron distribution in energy spectrum describes by density of states. Obtained total density states spectrum for α-Al_2O_3 and α-$Al_{1.5}Mn_{0.5}O_3$ with spin-up and down have been shown in Figure 5. In this situation, like band structure, because of adding Mn magnetic impure to Alumina, the energy gap decreases. This reduction is

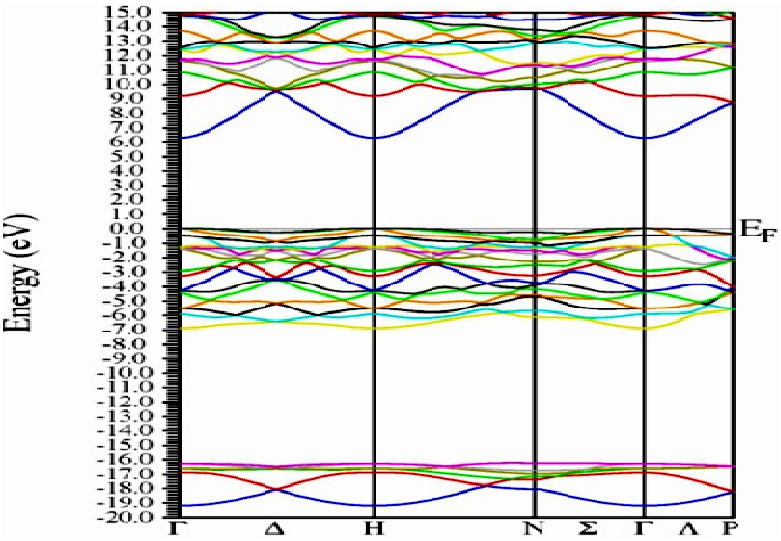

Figure 2. Calculated electronic band structure for α –Al_2O_3.

Table 2. Calculated band gaps for Al_2O_3 and $Al_{1.5}Mn_{0.5}O_3$.

	Present (eV)	Theory (eV)	Experiment (eV)
Al_2O_3	6.3	6.4	8.7
$Al_{1.5}Mn_{0.5}O_3$(up)	0.6	-	-
$Al_{1.5}Mn_{0.5}O_3$(down)	3.7	-	-
$Al_{1.5}Mn_{0.5}O_3$ (without spin polarization)	2.5	-	-

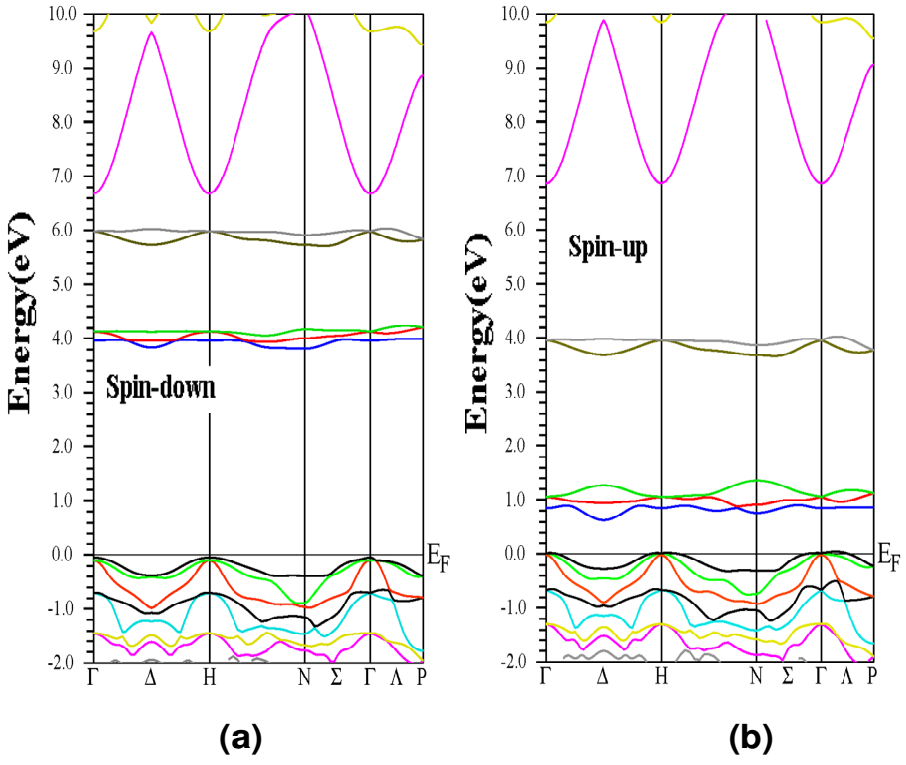

Figure 3. Calculated band structure for $Al_{1.5}Mn_{0.5}O_3$ with (a) spin up and (b) spin down.

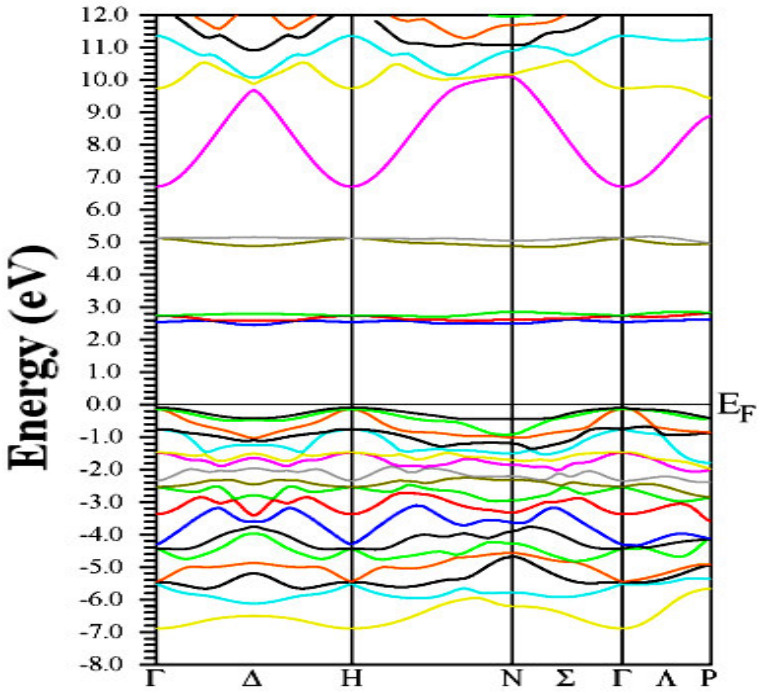

Figure 4. Calculated band structure for $Al_{1.5}Mn_{0.5}O_3$ without spin polarization effect.

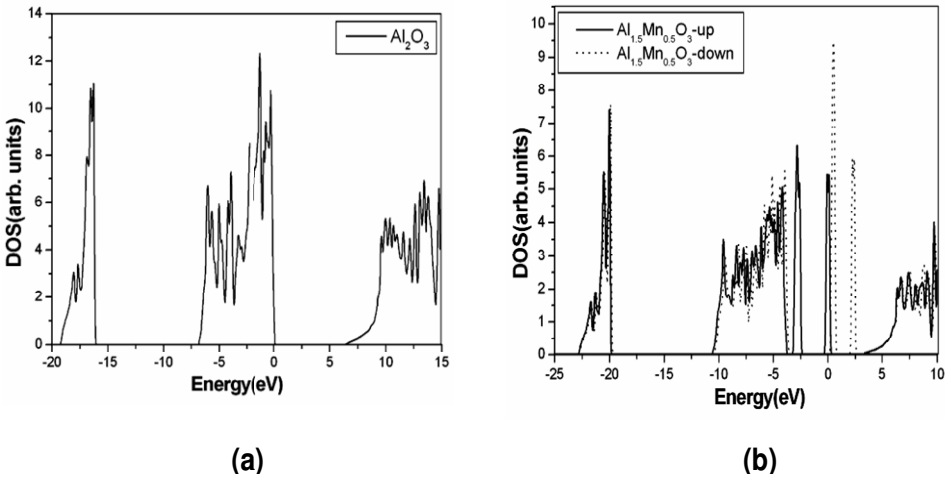

Figure 5. Calculated total density of state for (a) α- Al_2O_3 and (b) for α-$Al_{1.5}Mn_{0.5}O_3$ in spin up and down.

because of appearing d states of these elements at the bottom of conduction band. The partial density of states is shown in Figure 6 .The obtained results,shows that d states of Mn magnetic impure,in spin-up and down states, are existing in different energy levels. And a kind of spin splitting happens for them. In Figure 6, in energy range -20 to -25 eV, there is extended O 2s orbital. The most portions of Al 2p and Al 2s orbital's are in conduction band and the portion of O 2p is more at valence band. Density spectrum of partial states helps a lot, to explain the mechanism and the chemical nature of the hybridization between the elements of $Al_{1.5}Mn_{0.5}O_3$. According to the Figure, Al 2p, O 2p and Mn 3d orbitals have the most affect at valence and conduction bands, and the portion of other states is worthless. Also Al 2p, O 2p and Mn 3d orbital's have a good overlapping and can

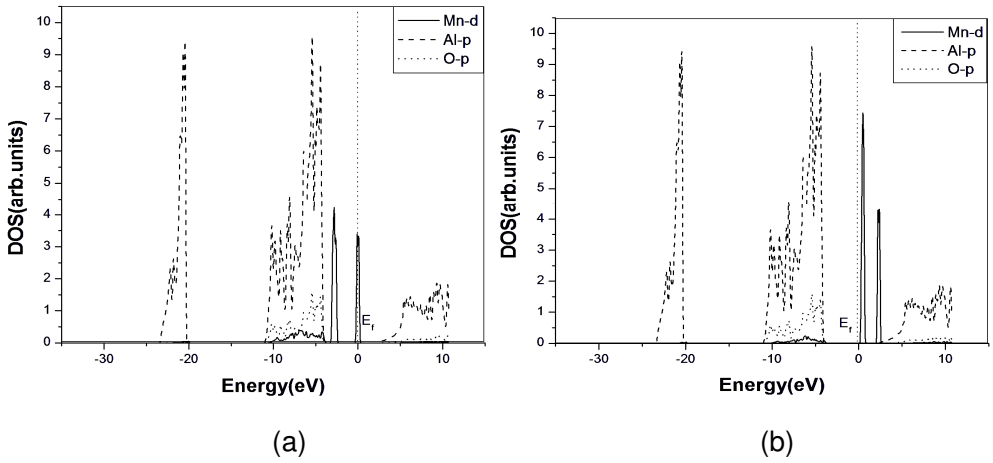

Figure 6. The partial density states for $Al_{1.5}Mn_{0.5}O_3$ in (a) spin up and (b) spin down.

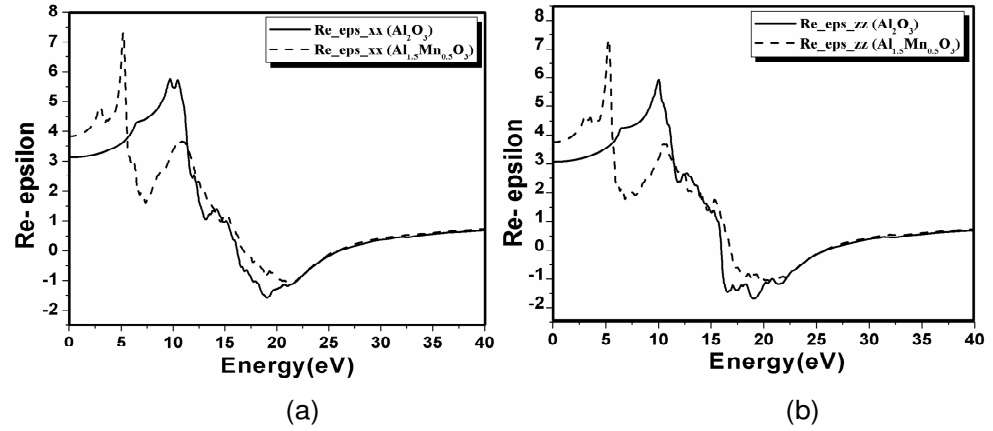

Figure 7. Calculated real part of dielectric function for α- Al_2O_3 and α-$Al_{1.5}Mn_{0.5}O_3$ (a) x-direction, and (b) z- direction.

have good hybridization together.

Optical results

Dielectric function

Transitions between occupied and unoccupied states, including plasmons and single particle excitations, are caused by the electric field of the photon. The dielectric function ε(ω), which describes the features of linear response of the system to an electromagnetic radiation, can be use in the following well-known relation (Hosseini et al., 2004):

$$\mathrm{Im}\varepsilon_{\alpha\beta}^{\{inter\}}(\omega)=\frac{\hbar^2e^2}{\pi m^2\omega^2}\sum_{c,v}\int d\mathbf{k}\langle c_k|p^{\alpha}|v_k\rangle\langle v_k|p^{\beta}|c_k\rangle\times\delta(\varepsilon_{ck}-\varepsilon_{vk}-\omega) \quad (1)$$

The interband expressions in the corresponding real parts are obtained by Kramers–Kronig transformation:

$$\mathrm{Re}_{\alpha\beta}^{\{inter\}}(\omega)=\delta_{\alpha\beta}+\frac{2}{\pi}P\int_0^{\infty}\frac{\omega'\,\mathrm{Im}\varepsilon_{\alpha\beta}(\omega')}{(\omega')^2-\omega^2}d\omega' \quad (2)$$

According to the symmetry of the crystal, the dielectric tensor may have up to two components (xx = yy and zz). The real part of the frequency dependent dielectric function for α-Al_2O_3 and α-$Al_{1.5}Mn_{0.5}O_3$ are shown in Figure 7 for x and z components. The static dielectric permittivity tensor, $\varepsilon_{\alpha\beta}(0)$, of a nonpolar material contains electronic (high frequency) and ionic contribution. The square of this value is equal to refractive index. The high frequency dielectric constant, ε(∞), and static refractive index are presented in Table 3. The results show that with the addition of Mn to alumina, refractive index increases; also this value is different for two components.

Table 3. Obtained high-frequency dielectric constants and static refractive index for α- Al_2O_3 and α-$Al_{1.5}Mn_{0.5}O_3$.

.

Direction	ℳ (∞)		n_0	
	α- Al_2O_3	α-$Al_{1.5}Mn_{0.5}O_3$	α- Al_2O_3	α-$Al_{1.5}Mn_{0.5}O_3$
This work:				
xx	3.11	3.85	1.76	1.96
zz	3.09	3.75	1.75	1.94
Experiment	3.17	-	1.78	-

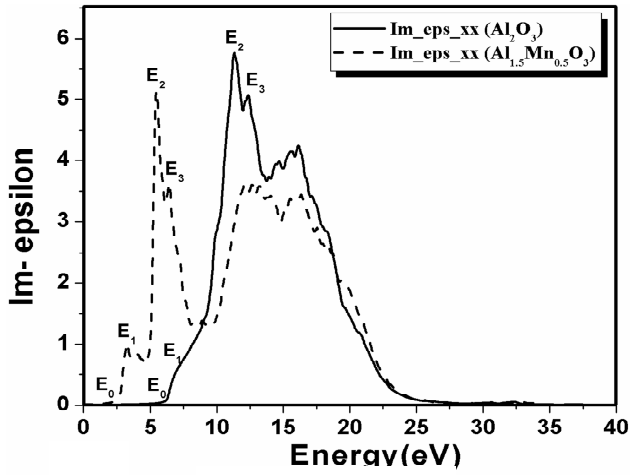

(a)

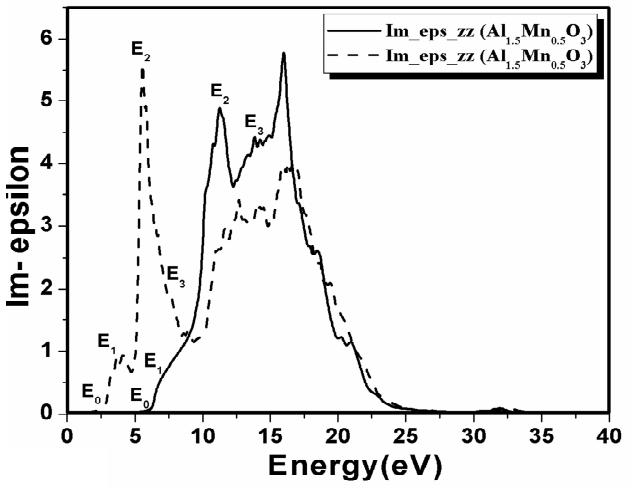

(b)

Figure 8. Calculated imagiary part of dielectric function for α-Al_2O_3 and α-$Al_{1.5}Mn_{0.5}O_3$ (a) x-direction, (b) z- direction.

Therefore, this compound is birefringent.The imaginary part of the frequency dependent dielectric function for α-Al_2O_3 and α- $Al_{1.5}Mn_{0.5}O_3$ are given in Figure 8 for x and z components. According to band structure (without spin polarization), the peaks on Im ε(ω) curves for these compounds (E_0, E_1, E_2, E_3) are related to the interband transitions from the valence to the conduction band states along Γ–Γ, Γ- P, Γ- H and Γ– N directions. For

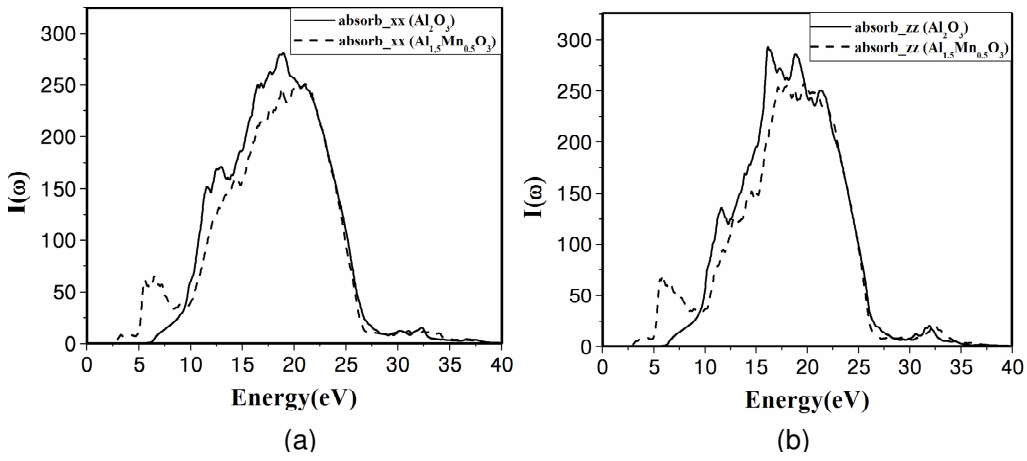

Figure 9. Calculated absorption for α- Al_2O_3 and α-$Al_{1.5}Mn_{0.5}O_3$ (a) x-direction, (b) z- direction.

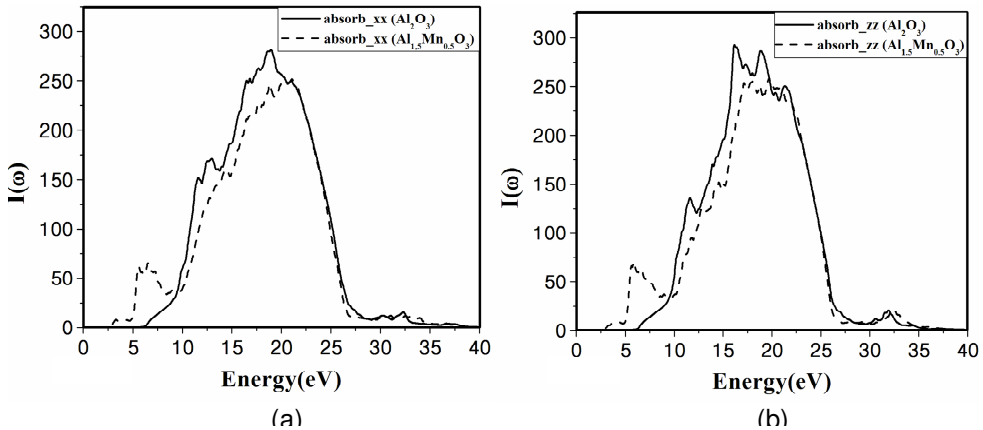

Figure 10. Calculated reflectivity for α- Al_2O_3 and α-$Al_{1.5}Mn_{0.5}O_3$ (a) x-direction ,(b) z- direction.

α-Al_2O_3, the electronic transitions are between the O-2p and Al- 3p in valence and conduction band states whereas, higher transitions are related to O-2s states. In the other hand for $Al_{1.5}Mn_{0.5}O_3$, Mn-3d states have important role in this transitions. It is clear for α-$Al_{1.5}Mn_{0.5}O_3$ that energy range of these peaks changed so that new peaks are created. These new peaks originate from created new states in band gap. Therefore electronic transitions for $Al_{1.5}Mn_{0.5}O_3$ are different with pure α-Al_2O_3.

Absorption

For calculating of absorption, we used the following relation:

$$\alpha_{\alpha\beta}(\omega) = \frac{2\omega k_{\alpha\beta}(\omega)}{c} \quad (3)$$

Figure 9 shows the calculated absorption for pure α-Al_2O_3 and α-$Al_{1.5}Mn_{0.5}O_3$. The absorption coefficient α(ω) is very large (about 10^4 cm^{-1}) and increases rapidly in the low energy region.The absorption edge of alumina begin in 6.2 eV but in $Al_{1.5}Mn_{0.5}O_3$ begin in 2.9 eV .The maximum absorption of α-Al_2O_3 occurs at 19.02 and 16.20 eV whereas for $Al_{1.5}Mn_{0.5}O_3$ occurs at 18.86 and 17.92 eV for x and z directions, respectively. With adding Mn, the maximum peak shifted to lower energy ranges at x direction and shifted to high energy ranges for direction. Mn impurity cause to create new peaks in absorption spectrum for α-Al_2O_3.

Reflectivity

Calculated reflectivity spectra for pure α-Al_2O_3 and α-$Al_{1.5}Mn_{0.5}O_3$ are given in Figure 10, which plot is in xx and zz directions. Optical reflection depends on incidence photon energy and it is plot in energy range of 0 to 35 eV.

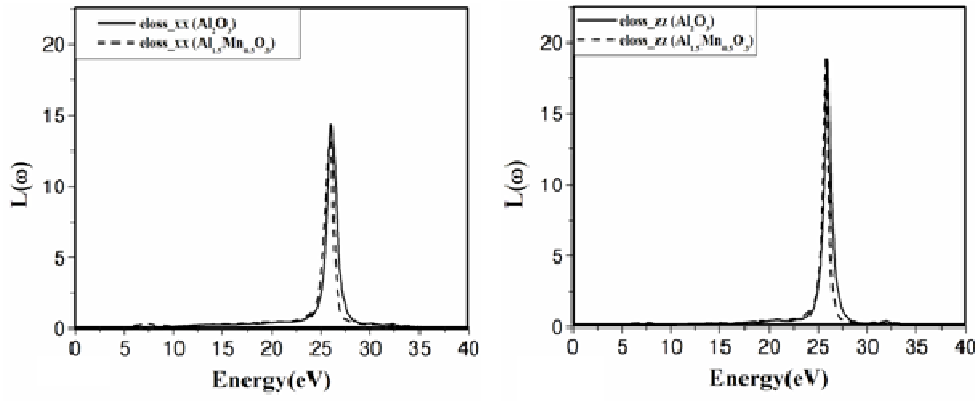

(a) (b)

Figure 11. Calculated EELS for α- Al_2O_3 and α-$Al_{1.5}Mn_{0.5}O_3$ (a) x-direction, (b) z- direction.

Table 4. Obtained plasmon energy for α- Al_2O_3 and α-$Al_{1.5}Mn_{0.5}O_3$ and compared with other results.

Direction	$\hbar\omega_p$	
	α- Al_2O_3	**α-$Al_{1.5}Mn_{0.5}O_3$**
This work		
xx	26.09	26.00
zz	25.93	25.93
Others		
Experiment	26.0	-
Theory	21.4	-

Obtained reflectivity in low energy is small so that it is increases and this increase oscillates .It gets maximum between 22.5 to 25 eV energy ranges in zz direction and this value is larger than x direction. Adding Mn to alumina cause to reflectivity increases at low energy (about 0 to 6 eV) and decreases at high energy (about 6 to 40 eV).

Electron energy loss spectroscopy (EELS)

EELS is a valuable tool for investigating various aspects of materials (French et al., 1998). It has important role in the materials design related to dielectric. Also these spectroscopes have the advantage of covering the complete energy range including non-scattered and elastically scattered electrons (zero loss), electrons that excite an atom's outer shell (valence loss) or valence interband transitions. Also the fast electrons excite the inner shell electrons (core loss) or induce core level excitation of near edge structure (ELNES) and XANES. In the case of interband transitions, this consists mostly of plasmon excitations. The scattering probability for volume losses is directly connected to the energy loss function. One can then calculate the EEL spectrum from the following relations (Yourdshahyan et al., 1997):

$$\text{EEL spectrum} = L(\omega) = \mathrm{Im}\left\{\frac{-1}{\varepsilon_{\alpha\beta}(\omega)}\right\} \quad (3)$$

In Figure 11, the energy loss function is plotted for α-Al_2O_3 and α-$Al_{1.5}Mn_{0.5}O_3$ for x and z directions in the energy range 0 to 40 eV. There is no energy loss for α-Al_2O_3 up to 6.36 eV and for $Al_{1.5}Mn_{0.5}O_3$ up to 2.56 eV energy range.

The short peaks before 25 eV in energy loss of Alumina relates to the transition from O-2p,Al-3p and peaks between 25 to 30 eV relates to the transition from O-2s and Al-3s to conduction band . The energy of the main maximum of Im $[-\varepsilon^{-1}(E)]$ is assigned to the energy of volume Plasmon $\hbar\omega_p$. The values of $\hbar\omega_p$ obtained in this work are given in Table 4. It is clear that, Mn impurity have not significant influence on Plasmon energy of α-$Al_{1.5}Mn_{0.5}O_3$. Obtained results are in good agreement with others.

Conclusion

We have calculated the structural, electronical and optical properties of α-Al_2O_3 and α-$Al_{1.5}Mn_{0.5}O_3$ using the full potential-linearized augmented plane wave (FP-LAPW) method with the generalized gradient approximation (GGA). The calculations show with adding Mn magnetic impurity to α-Al_2O_3 the energy gap reduces. According to the atomic configuration of Mn ($[Ar]3d^5 4s^2$), d levels of these elements are half-full so that the results show that band gap is different for spin-up and down (spin splitting effect). Obtained results show two static refractive index 1.76, 1.75 and two plasmon energy, 26.09 and 25.93 eV for x and z directions, respectively. The substitution of Mn for Al increases the static refractive index to 1.96 and 1.94 for α-$Al_{1.5}Mn_{0.5}O_3$ for x and z directions, respectively, and this is mainly due to the number of states originating from the Mn-d state in the conduction band.

ACKNOWLEDGEMENTS

We thank Professor P. Blaha, Vienna University of Technology Austria, for help with technical assistance of using Wien2k package.

REFERENCES

Ahuja R, Osorio-Guillen J, Almeida J, Holm B, Ching W, Johansson B (2004). Electronic and optical properties of γ-Al_2O_3 from *ab initio* theory. J. Phys. Condens. Matter, 16: 2891.

Blaha P, Schwarz K, Madsen G, Kvasnicka D, Luitz J (2011). Institute of Mater. Chem.TU Vienna, http://www.wien2k.at/.

Chatterjee A, Niwa S, Mizukami F (2005). Structure and property correlation for Ag deposition on α-Al_2O_3 a first principle study. J. Mol. Graphics Model., 23: 447-456.

French R, Mullejans H, Jones DJ (1998). Optical properties of aluminum oxide: determined from vacuum ultraviolet and electron energy loss spectroscopy. Am. Ceram. Soc., 81: 2549-2557.

Hohenberg K, Kohn S (2011). Density functional theory (DFT): Spring Quart., 2011.

Hosseini SM, Rahnamaye Aliabad HA, Kompany A (2004). Influence of La on electronic structure of α-Al_2O_3 high k-gate from first principle. Ceramics Int., 31: 671-675.

Yourdshahyan Y, Engberg U, Bengtsson L, Lundqvist B, Hammer B (1997). A theoretical investigation of the structure of k-Al_2O_3". Phys. Rev. B, 55: 8721.

Peterson M, Wanger F, Hufnagel S, Scheffler M, Blaha P, Schwarz K (2000). Improving the efficiency of FP-LAPW calculations. Compute. Phys. Commun., 126: 294-309.

Wang X, Padture N, Tanaka H, Ortiz A (2005). Wear-resistant ultra-fine-grained ceramics", Acta Mater., 53: 271–277.